CrossMark

ORIGINAL ARTICLE

Novel Cardiac Magnetic Resonance Feature Tracking (CMR-FT) Analysis for Detection of Myocardial Fibrosis in Pediatric Hypertrophic Cardiomyopathy

Soujanya Bogarapu[1] · Michael D. Puchalski[1] · Melanie D. Everitt[2] ·
Richard V. Williams[1] · Hsin-Yi Weng[3] · Shaji C. Menon[1]

Abstract Myocardial fibrosis is a risk factor for sudden cardiac death in hypertrophic cardiomyopathy (HCM) and is conventionally identified by cardiac magnetic resonance imaging (CMR) using late gadolinium enhancement (LGE). This study evaluates utility of a novel 16-segment CMR feature tracking (CMR-FT) technique for measuring left ventricular (LV) strain (S) and strain rate (SR) on non-contrast cine images to detect myocardial fibrosis in pediatric HCM. We hypothesized that CMR-FT-derived S and SR will accurately differentiate HCM patients with and without myocardial fibrosis. Consecutive children with HCM who underwent CMR with LGE at our institution from 2006 to 2014 were included. Global and regional longitudinal, radial and circumferential S and SR of the LV in 2D and 3D were obtained using a CMR-FT software. Comparisons were made between HCM patients with (+LGE) and without (−LGE) delayed enhancement. Of the 29 HCM patients (mean age 13.5 ± 6.1 years; 52 % males), 11 (40 %) patients (mean age 17.5 ± 8.4 years) had +LGE. Global longitudinal, circumferential and radial S and SR were lower in +LGE compared to −LGE patients, in both 2D and 3D. Regional analysis revealed lower segmental S and SR in the septum with fibrosis compared to free wall without fibrosis. A global longitudinal S of ≤ −12.8 had 91 % sensitivity and 89 % specificity for detection of LGE. In pediatric HCM patients with myocardial fibrosis, global LV longitudinal, circumferential and radial S and SR were reduced, specifically in areas of fibrosis. A global longitudinal S of ≤ −12.8 detected patients with fibrosis with high degree of accuracy. This novel CMR-FT technique may be useful to identify myocardial fibrosis and risk-stratify pediatric HCM without use of contrast agents.

Keywords Hypertrophic cardiomyopathy · Myocardial fibrosis · Cardiac magnetic resonance imaging · Feature tracking analysis · Strain and strain rate

Abbreviations
CMR   Cardiac magnetic resonance
FT   Feature tracking
HCM   Hypertrophic cardiomyopathy
LGE   Late gadolinium enhancement
LV   Left ventricle
SCD   Sudden cardiac death
SSFP Steady-state free precession
S   Peak systolic strain
SR   Peak systolic strain rate
TDI   Tissue Doppler imaging

✉ Shaji C. Menon
  shaji.menon@hsc.utah.edu

1   Division of Pediatric Cardiology, Department of Pediatrics, University of Utah, 81 N Mario Capecchi Drive, Salt Lake City, UT 84113, USA

2   Division of Pediatric Cardiology, Children's Hospital Colorado, Aurora, CO, USA

3   Study Design and Biostatistics Center, University of Utah School of Medicine, Salt Lake City, UT, USA

Introduction

Hypertrophic cardiomyopathy (HCM) is the most common heritable cardiovascular disorder with a population prevalence of 1:500 and is a leading cause of sudden cardiac death (SCD) in young [4, 23]. Myocardial fibrosis is

🖄 Springer

commonly seen in HCM and is associated with ventricular tachyarrhythmias, diastolic dysfunction, heart failure and SCD [4, 9, 36, 40, 41].

Late gadolinium enhancement (LGE) on cardiac magnetic resonance imaging (CMR) is the reference standard for noninvasive assessment of myocardial fibrosis in HCM [1, 25]. CMR-derived LGE is an independent risk factor for adverse cardiac events in HCM patients [5, 8, 27]. Despite a favorable safety profile, the use of gadolinium-based contrast agents (GBCA) mandates placement of an intravenous line, increases scan time and is contraindicated in patients with impaired renal function. In addition to the more common reports of allergy and anaphylactic shock seen with contrast agents, GBCA is specially associated with a rare but debilitating condition—nephrogenic systemic fibrosis in patients with renal insufficiency and multiorgan dysfunction [10].

Recently, CMR myocardial feature tracking (FT), a technique similar to echocardiographic speckle tracking, has been described [22]. CMR-FT allows the tracking of tissue voxel motion of CMR cine steady-state free precession (SSFP) images to derive wall mechanics and strain (S) without acquisition of additional sequences [17]. CMR-FT has been validated against traditional myocardial tagging methods with good agreement between CMR-FT and harmonic phase imaging [3, 16]. Recently, its use in determining quantitative wall motion assessment for the detection of transmural scar in post myocardial infarction patients as well as for identification of myocardial fibrosis in patients with Duchenne muscular dystrophy has been demonstrated [21, 32, 33]. To date, no comparable studies have assessed the utility of CMR-FT for the detection of LGE in patients with HCM. In the current study, we sought to apply a novel 16-segment CMR-FT technique of left ventricular (LV) S and strain rate (SR) on non-contrast cine MR images to detect myocardial fibrosis as defined by LGE-CMR in pediatric HCM. We hypothesized that CMR-FT-derived S and SR will accurately differentiate subjects with and without myocardial fibrosis.

Materials and Methods

Study Cohort

This single-center retrospective cohort study included all consecutive HCM subjects <25 years of age with phenotypic or genotypic HCM who underwent clinically indicated CMR with LGE at our institution between January 2006 and December 2014. HCM was defined as a positive genetic test result for a mutation known to be associated with HCM or the presence of echocardiographic findings including asymmetric septal hypertrophy, septal hypertrophy with systolic anterior motion of the mitral valve or total left ventricular mass >2 standard deviations above the mean for body surface area without an identifiable cause [13]. Those with coexisting congenital heart disease, an underlying syndrome or storage disorder predisposing to secondary HCM were excluded. The institute's CMR database was used to identify the study cohort. This study was approved by our institutional review board.

Patient medical records were reviewed for demographic data, family history, New York Heart Association (NYHA) functional class, implantable cardioverter-defibrillator placement (ICD) and genetic testing.

CMR Imaging

CMR Imaging Protocol

CMR studies were performed on a 1.5-T GE (General Electric Healthcare; Milwaukee, WI, USA) system, with an appropriate torso or cardiac-phased array coils according to body size. All studies were performed utilizing breath-holding when possible, to limit motion artifact. For subjects who could not adequately breath-hold, a free breathing technique with multiple signal averaging was used. Following a three-plane localizer, electrocardiogram-triggered segmented k-space fast-spoiled gradient-recalled cine sequences (SSFP) were performed in two- and four-chamber planes followed by 12 contiguous short-axis slabs perpendicular to the long axis of the left and right ventricle from base to apex (slice thickness 6–8 mm, interslice space 0–2 mm). LGE imaging was performed using inversion recovery prepared gradient-echo sequence 8–10 min after intravenous bolus of 0.2-mmol/kg GBCA in the short-axis and four-chamber planes [30].

Ventricular Volumetry and Global Functional Data

Ventricular volumes, mass and global function were assessed via standard planimetry techniques using semi-automated commercially available computer software (QMASS v.6.1.6, Medis Medical Imaging Systems, Netherlands). LV volumes, ejection fraction and myocardial mass were measured, and presence and absence of LGE and its location were recorded. End-diastolic and end-systolic phases were selected manually, with end-diastole defined as the phase with the largest right ventricular (RV) and LV area and end-systole as the phase with the smallest RV and LV area. Tracing was performed manually on each end-diastolic and end-systolic short-axis view. Ejection fraction for each ventricle was calculated by the following equation $EF = EDV - ESV/EDV$. The epicardial borders of the LV and RV were outlined at end-diastole for determination of ventricular mass

CMR-FT Analysis

CMR-FT analysis was performed using a novel commercially available software (cvi^{42} version 5, © Circle Cardiovascular Imaging Inc., Calgary, Alberta, Canada). Two- and four-chamber and short-axis images were uploaded into the software which reconstructs a 3D model that is used for analysis of 2D and 3D longitudinal, radial and circumferential S and SR. The preferred images were loaded into the analysis/viewer frame of the software and analyzed in a random order by two investigators (SB, SM) blinded to the MRI findings. FT analysis was done manually by delineating the endocardial and epicardial surface in end-diastolic phase. Short-axis stacked slices were used to analyze the apical, mid-ventricular and basal LV longitudinal, radial and circumferential S and SR in 2D and 3D. For a regional and global analysis of S and SR and the generation of polar map views, a short-axis reference point was manually defined at the RV upper septal insertion of the LV. Analysis of the S and SR was computed automatically in all slices by the software in 2D as well as 3D (Fig. 1).

We used the software to analyze S and SR results, in both 2D and 3D, using the AHA 17-segment model for assessment of regional and global myocardial mechanics in our subjects [7, 30]. Due to inconsistent tracking of cardiac apex and absence of apical HCM subjects in this cohort, we excluded the apex and used a 16-segment model (six basal, six mid ventricular and four apical segments) for the study.

Global S and SR measurements were calculated by software using the average of the peak values of the 16 segments, for both 2D and 3D models.

Statistical Analysis

Data are presented as mean ± SD or median (IQR) depending on the assumption of normality. Categorical variables are summarized using frequency and percentage. Comparisons of demographic, clinical, echocardiographic and CMR characteristics between the LGE and no-LGE groups were performed using T test or Wilcoxon sign rank test for continuous scale of measurements and Fisher's exact test for categorical variables. Statistical significance was defined as a p value <0.05. Regional myocardial deformation for the septum versus lateral free wall was compared using the average of basal and mid-ventricular septal and lateral segments, respectively. Evaluation of the distribution of S and SR at basal septal versus basal free wall among +LGE and −LGE cohorts were performed using target plot analysis [24].

The accuracy of the diagnostic test (S and SR) is measured using sensitivity, specificity, positive predictive valve (PPV) and negative predictive valve (NPV). Receiving operating characteristics (ROC) curve analysis was used to determine optimal cutoff value to predict presence or absence of LGE among subjects with HCM.

For the purpose of analyzing the relationship between segmental S/SR and LGE, we divided the 3D septal
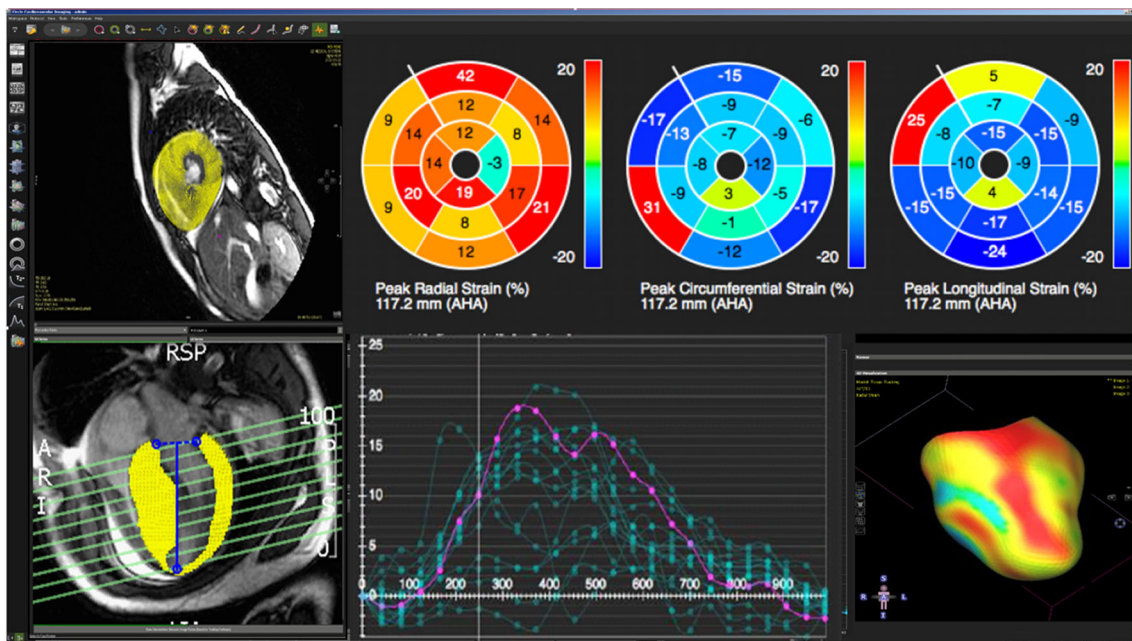
Fig. 1 Color map of CMR-FT-derived 3D S and SR in 16-segments and 3D LV model depicting reduced strain in the hypertrophied septum (*blue* and *yellow area in right lower corner image*). *CMR* cardiac magnetic resonance, *FT* feature tracking, *S* strain, *SR* strain rate

longitudinal S and SR into four quartiles; with quartile 1 including the least negative and most abnormal S and SR, and quartile 4 the most negative S and SR. Occurrence and distribution of LGE in each quartile was analyzed. All statistical analyses were performed using the SAS® 9.4 (SAS Inc. N.C. USA).

Results

A total of 29 HCM subjects (15, 52 % males) at a mean age of 13.5 ± 6.1 years at the time of their CMR were included in the study (Table 1). The majority of subjects were asymptomatic, with no subjects in NYHA class III or IV classes. All 29 subjects had normal LV systolic function with a mean ejection fraction of 74 ± 6.1 %. Apart from one subject with diffuse concentric hypertrophy, all other subjects had reverse septal HCM with the maximum LV wall thickness ranging from 13.5 mm to 52 mm. LGE was observed in 11 (40 %) subjects (mean age of 17.5 ± 8.4 years). Comparison based on the presence or absence of LGE (+LGE vs. −LGE groups) is outlined in Table 1. No differences were observed between the +LGE and −LGE groups in age, gender, body surface area, family history of HCM or past history of aborted SCD. Compared to −LGE subjects, +LGE subjects were more likely to have an ICD ($p = 0.04$).

CMR functional data of the entire cohort, and +LGE and −LGE cohorts are summarized in Table 2. There was no difference in CMR-derived LV and RV end-diastolic, end-systolic volumes and ejection fraction between the +LGE and −LGE cohorts. Subjects with LGE had more severe hypertrophy compared to those without, exhibiting significantly higher maximum LV wall thickness (34.4 ± 7.8 vs. 20.0 ± 6.3 mm, $p < 0.01$) and indexed LV mass z score (6.6 ± 4.1 vs. 2.8 ± 3, $p < 0.01$).

There were significant differences in peak systolic global and regional S and SR between the +LGE and −LGE cohorts (Table 3). Compared to −LGE subjects, +LGE subjects had lower global longitudinal, radial and circumferential S and SR, in both 2D and 3D by CMR-FT (Fig. 2). On ROC analysis, a global 3D longitudinal S of ≤ −12.8 predicted the presence of LGE with a sensitivity of 91 % (95 % CI 58.7–99.8 %), specificity of 89 % (95 % CI 65.3–98.6 %) and AUC of 0.899 (95 % CI 0.78–1.00), Fig. 3. Subjects with global 3D longitudinal S of ≤ −12.8 were 80 times more likely to have LGE (odds ratio 80.0, 95 % CI 6.39 to infinite, $p = 0.0007$).

Regional analysis of S and SR, likewise, yielded significant differences between the septum and LV free wall, in both 2D and 3D (Table 4). All +LGE subjects had markedly decreased longitudinal, radial and circumferential S and SR in the fibrotic septum compared to LV free wall without fibrosis ($p < 0.01$ for all) (Fig. 4). The distribution of LGE is summarized in Fig. 5. The anteroseptal and inferoseptal LV segments were most commonly involved (19/23, 83 %), followed by the anterior (2/23, 9 %) LV segments. One patient had involvement of the septum as well as LV free wall (1/23, 4 %). The relationship between segmental 3D longitudinal S and LGE is depicted in Fig. 6. The segments with LGE had the lowest segmental S values. In the lowest S quartile (quartile 1) 78 % had LGE. Figure 7 demonstrates the segmental differences in S between septal and LV free wall. The segmental longitudinal S was significantly reduced in areas with LGE (septum) compared to opposing non LGE segments in LV free wall.

Table 1 Demographics of cohort, +LGE and −LGE cohorts

Clinical characteristics	Total ($n = 29$)	+LGE ($n = 11$)	−LGE ($n = 18$)	p value
Age at CMR (years) (mean ± SD)	14.5 ± 7.4	17.4 ± 8.4	12.7 ± 6.3	0.096
Males (%)	15 (52 %)	7 (64 %)	8 (44 %)	0.316
Type of HCM				
Obstructive	9 (31 %)	5 (45 %)	4 (22 %)	
Non-obstructive	20 (69 %)	6 (55 %)	14 (78 %)	
Body surface area (m²) (mean ± SD)	1.51 ± 0.6	1.55 ± 0.5	1.49 ± 0.7	0.825
NYHA class				
Class I	21 (72 %)	9 (82 %)	12 (67 %)	
Class II	8 (28 %)	5 (18 %)	3 (33 %)	
Class III–IV	0			
Family history of HCM (%)	10 (36 %)	4 (40 %)	6 (33 %)	1.000
Family history of SCD (%)	7 (25 %)	2 (20 %)	5 (28 %)	1.000
Aborted SCD (%)	2 (7 %)	2 (20 %)	0	0.119
ICD placement (%)	11 (38 %)	7 (70 %)	4 (22 %)	0.020

CMR cardiac magnetic resonance, *HCM* hypertrophic cardiomyopathy, *NYHA* New York Heart Association, *ICD* intracardiac defibrillator, *SCD* sudden cardiac death

Table 2 CMR volumetric findings for the study cohort and +LGE versus −LGE cohorts

	Total (n = 29)	+LGE (n = 11)	−LGE (n = 18)	p value
CMR data				
LVEDVi (mL/m^2)	103.5 ± 41.9	110.4 ± 23.5	99.3 ± 50.3	0.43
LVESVi (ml/m^2)	38.1 ± 14.4	27.4 ± 10.8	27.5 ± 16.6	0.78
LV ejection fraction (%)	74 ± 6	72 ± 8	75 ± 6	0.15
LV mass z score	4.38 ± 3.9	6.6 ± 4.1	2.8 ± 3.1	<0.01
RV EDVi (ml/m$^{2)}$)	89.6 ± 41.9	82.7 ± 39.6	91.3 ± 23.7	0.981
RV ESVi (ml/m$^{2)}$)	40.1 ± 18	43.7 ± 16.1	41.4 ± 15.3	0.862

CMR cardiac magnetic resonance, *LGE* late gadolinium enhancement, *LV* left ventricle, *LVEDVi* left ventricular end-diastolic volume indexed to body surface area, *LVESVi* left ventricular end-systolic volume indexed to body surface area, *RVEDVi* right ventricular end-diastolic volume indexed to body surface area, *RVESVi* right ventricular end-systolic volume

Table 3 2D and 3D global radial, circumferential and longitudinal strain and strain rate for +LGE and −LGE cohorts

|	Total (n = 29)	+LGE (n = 10)	−LGE (n = 18)	p value
2D				
Strain				
Radial	25.6 ± 6	19.7 ± 3.8	29.1 ± 3.9	<0.0001
Circumferential	−16 ± 5.7	−12.2 ± 2.9	−18.9 ± 2.9	<0.0001
Longitudinal	−3.6 ± 3.3	−1.4 ± 1.1	−4.9 ± 3.5	0.0004
Strain rate				
Radial	172.2 ± 52.5	136.5 ± 24.7	195.3 ± 53.2	0.0003
Circumferential	−134.7 ± 33.5	−104.7 ± 16.5	−154.2 ± 26.4	<0.0001
Longitudinal	−32.5 ± 40.4	−9.7 ± 25.1	−47.3 ± 42.1	0.0003
3D				
Strain				
Radial	14.2 ± 4.8	9.3 ± 2.8	17.3 ± 2.7	<0.0001
Circumferential	−14.2 ± 3.3	−10.7 ± 2.1	−16.3 ± 1.7	<0.0001
Longitudinal	−13.2 ± 3.2	−9.9 ± 2.1	−15.1 ± 1.9	<0.0001
Strain rate				
Radial	112.3 ± 34.8	79.1 ± 11.9	133.8 ± 28.7	<0.0001
Circumferential	−117 ± 22.3	−95.1 ± 11.5	−131 ± 14.7	<0.0001
Longitudinal	−114.5 ± 24.4	−92 ± 17.2	−129.1 ± 15.6	<0.0001

LGE late gadolinium enhancement

Discussion

Our study demonstrates the ability of CMR-FT-derived S and SR to discriminate HCM patients with +LGE from −LGE. Unlike previous CMR-FT studies using single slice in various planes for evaluation of myocardial deformation, in this study we used a novel CMR-FT technique that uses the entire LV myocardium to generate an AHA 16-segment model of the entire LV for measurement of 2D and 3D S and SR [11, 18, 29, 43]. Our study has two key findings. First, +LGE patients had significantly reduced global 2D and 3D S and SR. Second, the area of myocardial fibrosis in the ventricular septum had the lowest segmental S and SR. These two findings makes this novel CMR-FT a promising technique for not only identifying patients with myocardial fibrosis but also helping localize the area of myocardial fibrosis based on segmental reduction in myocardial deformation without the need for GBCA. A global 3D longitudinal S cutoff value of ≤12.8 was associated with a high degree of accuracy for the detection of areas of myocardial fibrosis.

Myocardial deformation analysis evaluates ventricular mechanics by quantifying S and SR. Myocardial S is the normalized, dimensionless measure of deformation of a segment of myocardium in response to an applied force [14]. The myocardial segments being a 3D structure can deform along 3 planes (x-, y-, and z-axes), known as normal strains, and 6 shear strains. However, for practical purposes, a simplified linear strain model is commonly used in deformation analysis. S is defined by the change in length
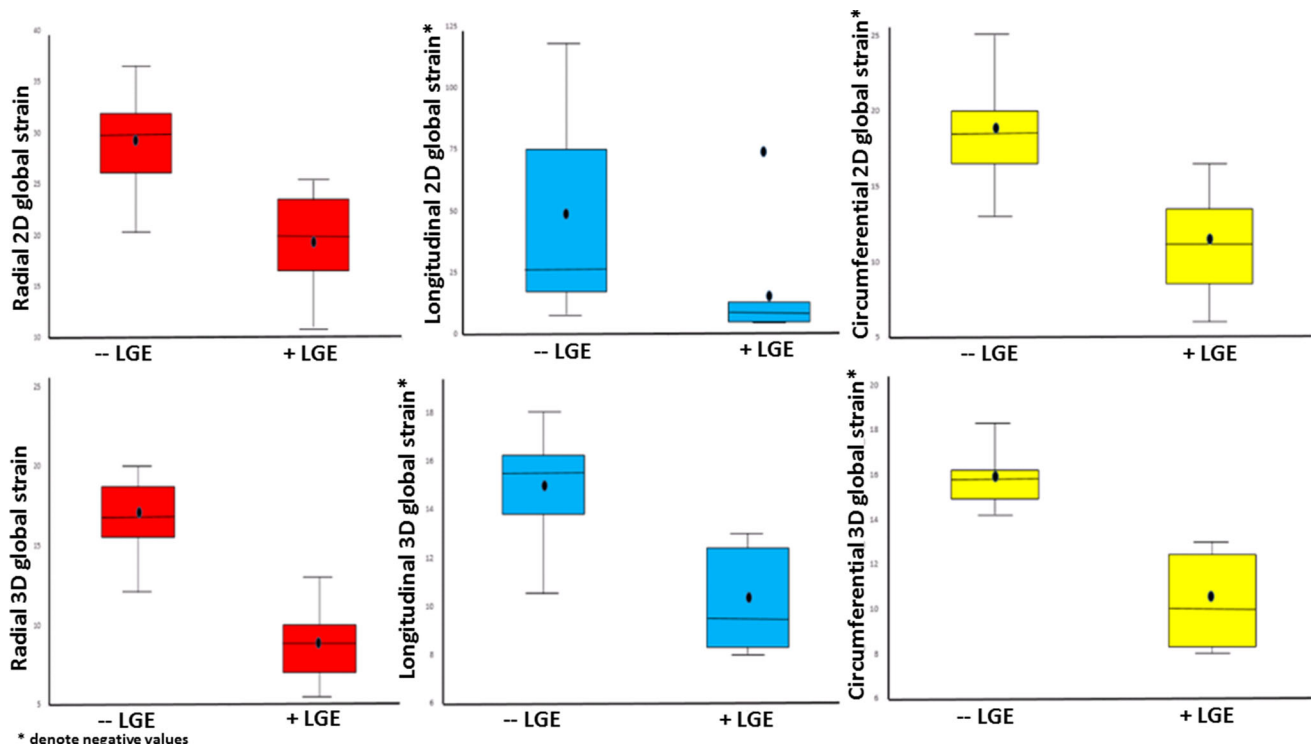
Fig. 2 Boxplots showing reduced 2D and 3D global radial, circumferential and longitudinal strain in +LGE compared to −LGE patients
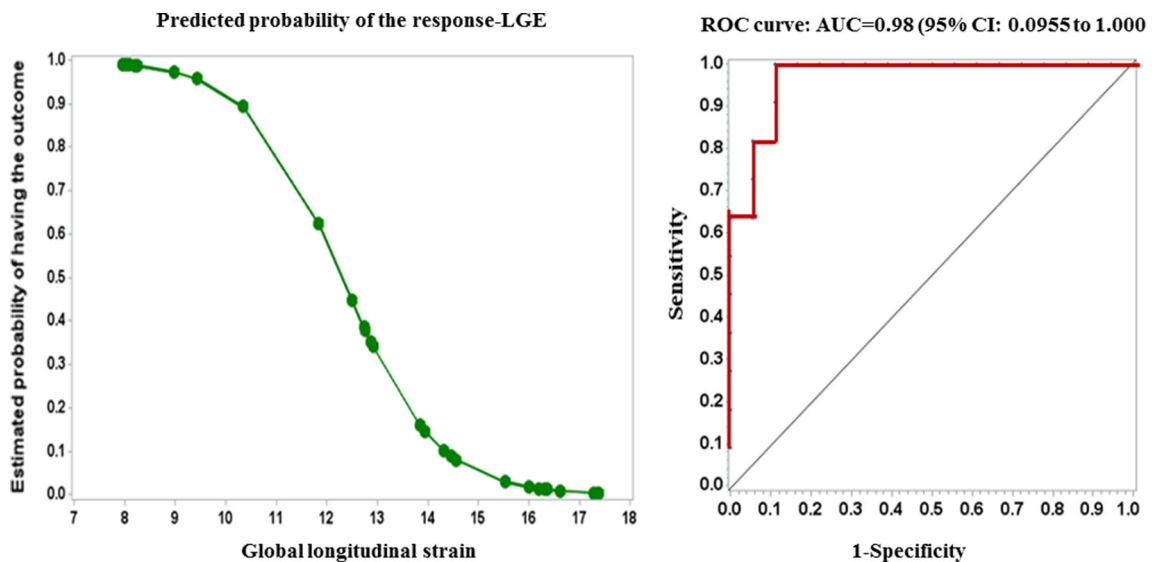
Fig. 3 Receiver operating characteristic (ROC) curve of 3D global longitudinal strain for detection of LGE

divided by the original length ($S = \Delta L / L0$, ΔL = change in length, and $L0$ = original length) [14]. S can be measured in longitudinal, radial and circumferential directions. S is a negative when the ventricle shortens longitudinally or circumferentially and is positive with radial thickening. SR, the time derivative of S, has been shown to correlate with left ventricular (LV) peak elastance, which is a load-independent global measure of ventricular systolic function

Table 4 2D and 3D regional radial, circumferential and longitudinal strain and strain rate for +LGE and −LGE cohorts

	Mean		+LGE	−LGE	p value
2D					
Strain	Septal	Radial	11 ± 2.8	19.1 ± 4.8	0.0003
		Circumferential	−8.2 ± 2.7	−14.1 ± 3.2	<0.0001
	Lateral	Radial	25.1 ± 6.3	33.2 ± 6.5	0.006
		Circumferential	−14.5 ± 5.1	−21.8 ± 3.7	0.0004
Strain rate	Septal	Radial	105.6 ± 30.8	153.6 ± 58	0.019
		Circumferential	−85.4 ± 18.2	−131 ± 43.5	0.0004
	Lateral	Radial	168 ± 31.6	221.3 ± 48.5	0.002
		Circumferential	−132.4 ± 22.9	−174.2 ± 32.5	0.001
3D					
Strain	Septal	Radial	6.3 ± 2.8	13.3 ± 3.9	<0.0001
		Circumferential	−8.2 ± 2.5	−13.2 ± 2.5	<0.0001
		Longitudinal	−7.2 ± 1.9	−12.2 ± 2.5	<0.0001
	Lateral	Radial	12.6 ± 3.4	20 ± 4	<0.0001
		Circumferential	−11.8 ± 3	−19 ± 3	0.0006
		Longitudinal	−11.5 ± 3.5	−17.1 ± 2.5	0.0002
Strain rate	Septal	Radial	61.3 ± 13.7	102.7 ± 36.2	<0.0001
		Circumferential	−75.8 ± 16.4	−108.1 ± 16.8	0.0002
		Longitudinal	−70.4 ± 23	−105.6 ± 27	0.0006
	Lateral	Radial	95.1 ± 14	153.6 ± 33.5	<0.0001
		Circumferential	−111 ± 16.7	−144.8 ± 22.6	0.0008
		Longitudinal	−105.5 ± 14.2	−147 ± 19.6	<0.0001

LGE late gadolinium enhancement

Fig. 4 Vector plot of mean 3D longitudinal strain in the basal segments demonstrating reduced strain in all segments in +LGE compared to −LGE. Septal strain was lower compared to lateral wall in the entire cohort; however, it was more pronounced in +LGE (*arrow*)
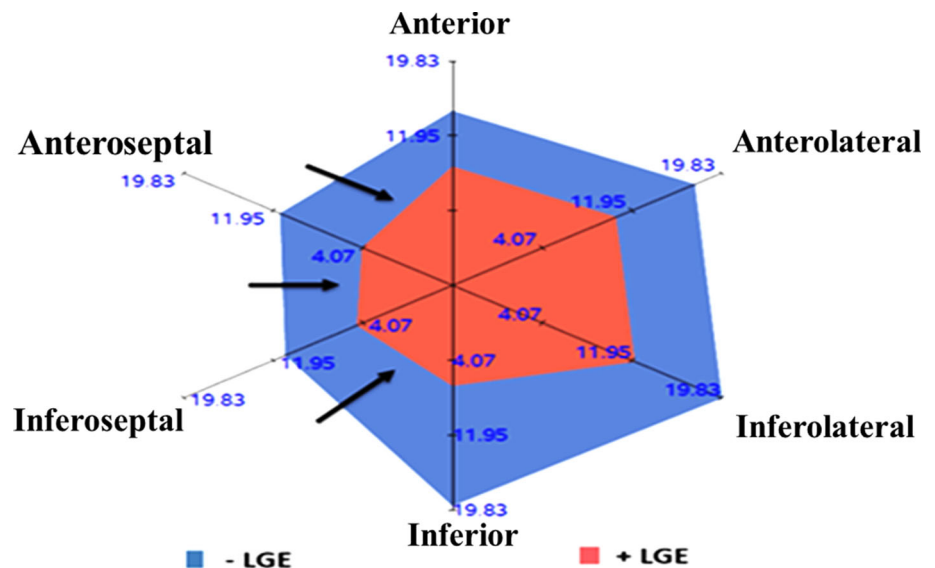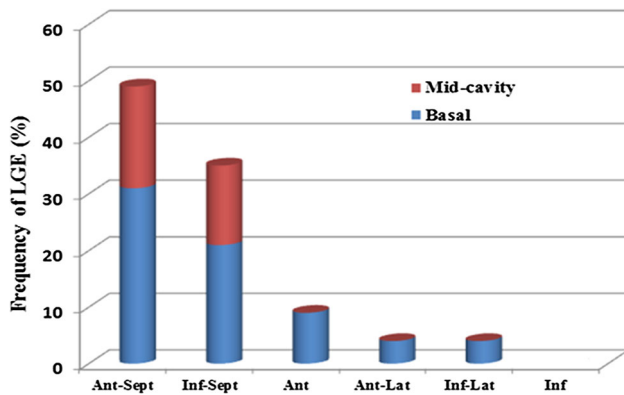
Fig. 5 Distribution of LGE in basal and mid-cavity. The *bar graph* shows anteroseptal, inferoseptal and anterior predominance of LGE, as well as the distribution of LGE between basal and mid-cavity segments. *LGE* late gadolinium enhancement, *Ant-Sept* anteroseptal, *Inf-Sept* inferoseptal, *Ant* anterior, *Ant-Lat* anterolateral, *Inf-Lat* inferolateral, *Inf* inferior

[15]. Various techniques have been used for S and SR analysis, including tissue Doppler imaging, speckle tracking imaging and myocardial tagging with CMR. CMR-FT is a novel technique for quantitative wall motion assessment from routinely available steady-state free precession (SSFP) cine sequences. Reasonable agreement between speckle tracking and CMR-FT has been demonstrated [28]. Furthermore, CMR-FT agrees well with myocardial

tagging, which is considered the reference standard for CMR quantitative wall motion assessment, but the former does not require the acquisition of additional sequences [16, 32]. Since its introduction in 2009, CMR-FT has found widespread clinical and research applications in various adult and congenital disorders [6, 19, 20, 28, 33]. Excellent intra- and interobserver reproducibility has been demonstrated for CMR-FT-derived variables [26, 39]. LV deformation myocardial mechanics are altered in HCM, with both hypertrophy and fibrosis contributing to regional and global impairment of myocardial shortening.

Regional heterogeneity of LGE in HCM is well documented in previous echocardiographic studies, occurring primarily in a mid-myocardial pattern, typically in hypertrophied areas of the septum with minimal LGE in the lateral wall and apex [12, 31]. Similar to previous studies, we found that LGE predominantly involved anterior and inferior septal segments and the lateral segments were involved less frequently and only in patients with significant LV septal involvement. These study findings are in line with previous echocardiographic studies using TDI and speckle tracking technology that illustrate reduced deformation in the septum versus lateral free wall in HCM patients. Weidemann et al. were the first to demonstrate decreased longitudinal mid-septal S and SR in a case report of a child with nonobstructive HCM, using TDI-derived S [42]. Subsequently, Sengupta et al. and Yang et al. [34, 43]
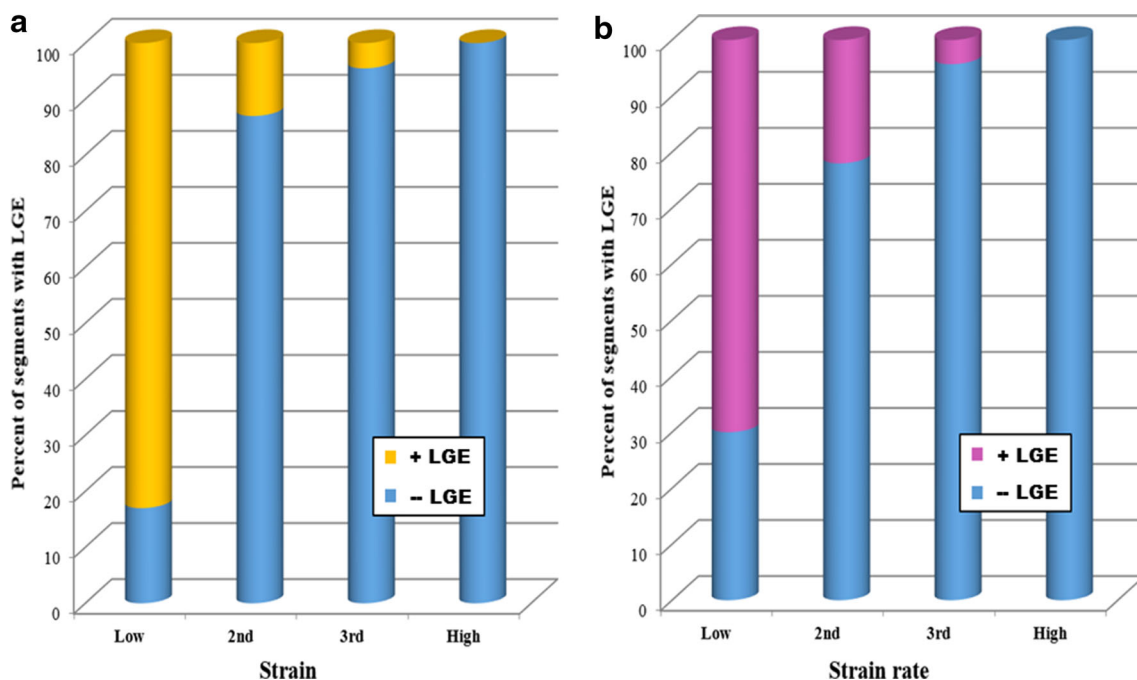

Fig. 6 Distribution of segmental LGE by quartile of CMR longitudinal 3D strain and strain rate. **a** No segments with strain or strain rate in the fourth (most negative) quartile had LGE. **b** LGE was unlikely in segments with highest strain and strain rate. LGE was most

common in the two lowest (most dysfunctional) strain and strain rate quartiles. 1st quartile = least negative strain and strain rate (most dysfunctional); 4th quartile = most negative strain and strain rate

Fig. 7 Distribution of segmental LGE by quartile of CMR longitudinal strain and strain rate. Increased proportion of LGE was noted in septal segments versus LV free wall based on analysis of all 348 segments. 1st quartile = least negative strain and strain rate (most dysfunctional); 4th quartile = most negative strain and strain rate
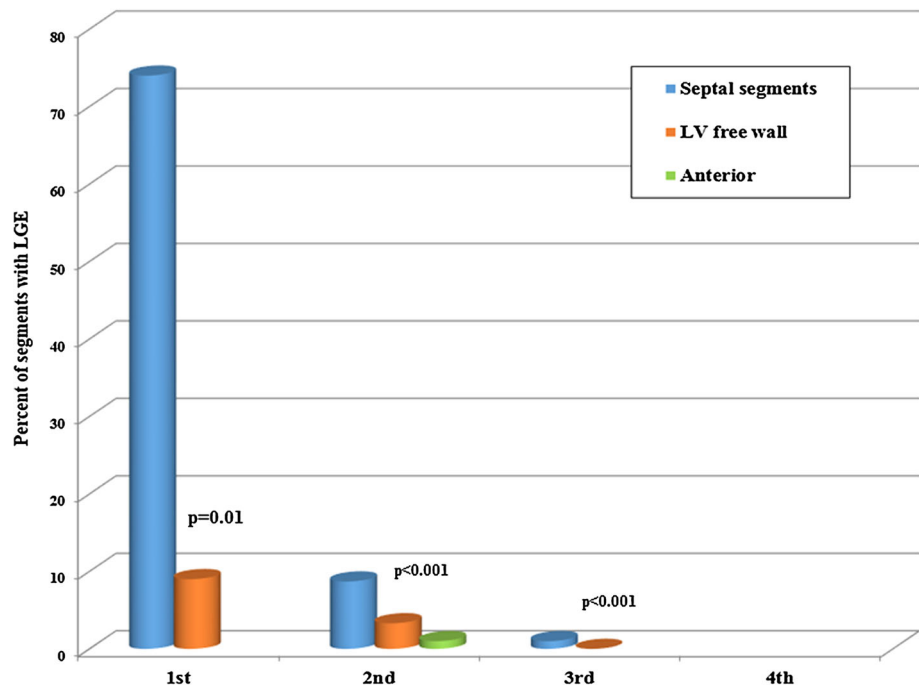
reported the assessment of regional myocardial function in adults with HCM, and found significantly reduced S in the septal segments of HCM compared with controls. Similar observations have been found in studies by Almaas et al. and Serri et al. [2, 35] using speckle tracking imaging. The advantages of using CMR-FT over echocardiography-derived S and SR imaging include (1) excellent differentiation between myocardial and blood pool, (2) excellent reproducibility, (3) high potential to be integrated in clinical practice since it can be performed on routine cine SSFP images without the need for time-consuming analysis and additional acquisition procedures and (4) validation with traditional CMR deformation analysis using tagged harmonic phase (HARP) analysis [16].

Our study demonstrates that the fibrotic septal myocardial segments can be differentiated from the corresponding non-fibrotic segments using CMR-FT-derived S and SR. There is scant evidence of utility of CMR-FT in this population. Smith et al. [38], in a series of 54 patients (30 HCM patients and 24 controls), demonstrated the ability of CMR-FT in analyzing differences in S. Segments with LGE were shown to have decreased longitudinal, radial and circumferential S in basal and mid-segments. However, unlike our study, when all segments were compared regardless of level, segments with LGE trended toward decreased radial S only versus segments without LGE, with no difference noted in circumferential and longitudinal S. We demonstrate a significant reduction in longitudinal, radial and circumference S and SR in segments with LGE, compared to segments without LGE. Compared to previous CMR-FT

studies that utilizes single slices, our study is unique in incorporation of the entire LV in its three dimensions for generating a 16-segment model of the LV for analysis of 2D and 3D regional and global myocardial deformation as well as for evaluation of its association with LGE.

CMR-derived LGE has proven valuable in predicting adverse cardiovascular events in adults with HCM [5, 8, 27]. Literature regarding clinical significance of CMR-derived LGE in pediatric HCM is limited. In a study of 50 children (mean age 14.1 ± 3.2 years), Smith et al. [37] demonstrated a positive association between extent of LGE and adverse clinical outcomes. Investigating the association between LGE and adverse clinical outcomes was not an aim of our study; however, all LGE segments could be differentiated from the non-LGE segments with high precision using CMR-FT-derived S and SR. Further prospective studies are necessary to confirm the findings of this pilot study and to evaluate the relationship between reduced deformation and clinical outcomes like SCD.

Our study is limited by its small sample size. The retrospective nature of the study limited the population to clinical referral for CMR allowing for potential selection bias. Although we found an increased incidence for ICD placement was noted in our patients with LGE, due to the retrospective nature of this study, we are unable to assess the long-term effect of abnormal S and SR on SCD. Owed to prior studies demonstrating reasonable intra- and interobserver reproducibility of CMR-FT technique, we did not conduct intra- and interobserver variability studies for CMR-FT in this study [26, 39].

Conclusions

This study illustrates the role of novel 2D and 3D CMR-FT-derived S and SR in demonstration of global and regional differences in myocardial deformation between those with and without LGE in HCM patients. These differences may be useful in predicting the presence and location of myocardial fibrosis in HCM without the need for GBCA. Further prospective studies to investigate the role of abnormal myocardial deformation in predicting clinical outcomes like SCD and heart failure are an important next step.

Compliance with Ethical Standards

Conflict of interest The authors have no conflicts of interest to disclose.

References

1. Almaas VM, Haugaa KH, Strom EH, Scott H, Smith HJ, Dahl CP, Geiran OR, Endresen K, Aakhus S, Amlie JP, Edvardsen T (2014) Noninvasive assessment of myocardial fibrosis in patients with obstructive hypertrophic cardiomyopathy. Heart 100:631–638

2. Almaas VM, Hauhaa KH, Strom EH, Scott H, Smith HJ, Dahl CP, Geiran OR, Endresen K, Aakhus S, Amlie JP, Edvardsen T (2014) Noninvasive assessment of myocardial fibrosis in patients with obstructive hypertrophic cardiomyopathy. Heart 100(8):631–638

3. Augustine D, Lewandowski AJ, Lazdam M, Rai A, Francis J, Myerson S, Noble A, Becher H, Neubauer S, Petersen SE, Leeson P (2013) Global and regional left ventricular myocardial deformation measures by magnetic resonance feature tracking in healthy volunteers: comparison with tagging and relevance of gender. J Cardiovasc Magn Reson 15:18

4. Basso C, Thiene G, Corrado D, Buja G, Melacini P, Nava A (2000) Hypertrophic cardiomyopathy and sudden death in the young: pathologic evidence of myocardial ischemia. Hum Pathol 31:988–998

5. Bruder O, Wagner A, Jensen CJ, Schneider S, Ong P, Kispert EM, Nassenstein K, Schlosser T, Sabin GV, Sechtem U, Mahrholdt H (2010) Myocardial scar visualized by cardiovascular magnetic resonance imaging predicts major adverse events in patients with hypertrophic cardiomyopathy. J Am Coll Cardiol 56:875–887

6. Buss SJ, Breuninger K, Lehrke S, Voss A, Galuschky C, Lossnitzer D, Andre F, Ehlermann P, Franke J, Taeger T, Frankenstein L, Steen H, Meder B, Giannitsis E, Katus HA, Korosoglou G (2014) Assessment of myocardial deformation with cardiac magnetic resonance strain imaging improves risk stratification in patients with dilated cardiomyopathy. Eur Heart J Cardiovasc Imaging 16:307–315

7. Cerqueira MD, Weissman NJ, Dilsizian V, Jacobs AK, Kaul S, Laskey WK, Pennell DJ, Rumberger JA, Ryan T, Verani MS (2002) Standardized Myocardial Segmentation and Nomenclature for Tomographic Imaging of the Heart. A statement for healthcare professionals from the cardiac imaging committee of the council on clinical cardiology of the American Heart Association. Circulation 105:539–542

8. Chan RH, Maron BJ, Olivotto I, Pencina MJ, Assenza GE, Haas T, Lesser JR, Gruner C, Crean AM, Rakowski H, Udelson JE, Rowin E, Lombardi M, Cecchi F, Tomberli B, Spirito P, Formisano F, Biagini E, Rapezzi C, De Cecco CN, Autore C, Cook EF, Hong SN, Gibson CM, Manning WJ, Appelbaum E, Maron MS (2014) Prognostic value of quantitative contrast-enhanced cardiovascular magnetic resonance for the evaluation of sudden death risk in patients with hypertrophic cardiomyopathy. Circulation 130(6):484–495

9. Choudary L, Mahrholdt H, Wagner A et al (2002) Myocardial scarring in asymptomatic or mildly symptomatic patients with hypertrophic cardiomyopathy. J Am Coll Cardiology 40:2156–2164

10. Elias J Jr, dos Santos AC, Koenigkam-Santos M, Nogueira-Barbosa MH, Muglia VF (2008) Complications from the use of intravenous gadolinium-based contrast agents for magnetic resonance imaging. Radiol Bras 41(4):263–267

11. Ennis DB, Epstein FH, Kellman P, Fananapazir L, McVeigh ER, Arai AE (2003) Assessment of regional systolic and diastolic dysfunction in familial hypertrophic cardiomyopathy using MR tagging. Magn Reson Med 50(3):638–642

12. Ganame J, Mertens L, Eidem BW, Claus P, D'Hooge J, Havemann LM, McMahon CJ, Elayda MA, Vaughn WK, Towbin JA, Ayres NA, Pignatelli RH (2007) Regional myocardial deformation in children with hypertrophic cardiomyopathy: morphologic and clinical correlations. Eur Heart J 28:2886–2894

13. Gersh BJ, Maron BJ, Bonow RO, Dearani JA, Fifer MA, Link MS, Naidu SS, Nishimura RA, Ommen SR, Rakowski H, Seidman CE, Towbin JA, Udelson JE, Yancy CW (2011) 2011 ACCF/AHA Guideline for the Diagnosis and Treatment of Hypertrophic Cardiomyopathy: a report of the American College of Cardiology Foundation/American Heart Association Task Force on Practice Guidelines. Developed in collaboration with the American Association for Thoracic Surgery, American Society of Echocardiography, American Society of Nuclear Cardiology, Heart Failure Society of America, Heart Rhythm Society, Society for Cardiovascular Angiography and Interventions, and Society of Thoracic Surgeons. J Am Coll Cardiol 58:e212–e260

14. Gorcsan J 3rd, Tanaka H (2011) Echocardiographic assessment of myocardial strain. J Am Coll Cardiol 58(14):1401–1413

15. Greenberg NL, Firstenberg MS, Castro PL, Main M, Travaglini A, Odabashian JA, Drinko JK, Rodriquez LL, Thomas JD, Garcia MJ (2002) Doppler-derived myocardial systolic strain rate is a strong index of left ventricular contractility. Circulation 105(1):99–105

16. Hor KN, Gottliebson WM, Carson C, Wash E, Cnota J, Fleck R, Wansapura J, Klimeczek P, Al-Khalidi HR, Chung ES, Benson DW, Mazur W (2010) Comparison of magnetic resonance feature tracking for strain calculation with harmonic phase imaging analysis. JACC Cardiovasc Imaging 3(2):144–151

17. Hor KN, Baumann R, Pedrizzetti G, Tonti G, Gottliebson WM, Taylor M, Benson W, Mazur W (2011) Magnetic resonance derived myocardial strain assessment using feature tracking. J Vis Exp 48:2356–2361

18. Kim YJ, Choi BW, Hur J, Lee HY, Seo JS, Kim TH, Choe KO, Ha JH (2008) Delayed enhancement in hypertrophic cardiomyopathy: comparison with myocardial tagging MRI. J Mag Reson Imaging 27(5):1054–1060

19. Kowallick JT, Lamata P, Hussain ST, Kutty S, Steinmetz M, Sohns JM, Fasshauer M, Staab W, Unterberg-Buchwald C, Bigalke B, Lotz J, Hasenfub G, Schuster A (2014) Quantification of left ventricular torsion and diastolic recoil using cardiovascular magnetic resonance myocardial feature tracking. PLoS ONE 9:e109164

20. Kutty S, Rangamani S, Venkataraman J, Li L, Schuster A, Fletcher SE, Danford DA, Beerbaum P (2012) Reduced global longitudinal and radial strain with normal left ventricular ejection fraction late after effective repair of aortic coarctation: a CMR feature tracking study. Int J Cardiovasc Imaging 29:141–150

21. Lang SM, Shugh S, Mazur W, Sticka JJ, Rattan MS, Jefferies JL, Taylor MD (2015) Myocardial fibrosis and left ventricular dysfunction in Duchenne muscular dystrophy carriers using cardiac magnetic resonance imaging. Pediatr Cardiol 36(7):1495–1501. doi:10.1007/s00246-015-1192-7.

22. Maret E, Todt T, Brudin L, Nylander E, Swahn E, Ohlsson JL, Engvall JE (2009) Functional measurements based on feature tracking of cine magnetic resonance images identify left ventricular segments with myocardial scar. Cardiovasc Ultrasound 16(7):75. doi:10.1186/1476-7120-7-53

23. Maron BJ (2002) Hypertrophic cardiomyopathy: a systematic review. JAMA 287:1308–1320

24. Menon SC, Erickson LK, McFadden M, Miller DV (2013) Effect of ventriculotomy on right-ventricular remodeling in hypoplastic left heart syndrome: a histopathological and echocardiographic correlation study. Pediatr Cardiol 34(2):354–363

25. Moon JC, McKenna WJ, McCrohon JA, Elliott PM, Smith GC, Pennell DJ (2003) Toward clinical risk assessment in hypertrophic cardiomyopathy with gadolinium cardiovascular magnetic resonance. J Am Coll Cardiol 41:1561–1567

26. Morton G, Schuster A, Jogiya R, Kutty S, Beerbaum P, Nagel E (2012) Inter-study reproducibility of cardiovascular magnetic resonance myocardial feature tracking. J Cardiovasc Magn Reson 14:43

27. O'Hanlon R, Grasso A, Roughton M, Moon JC, Clark S, Wage R, Webb J, Kulkarni M, Dawson D, Sulaibeekh L, Chandrasekaran B, Bucciarelli-Ducci C, Pasquale F, Cowie MR, McKenna WJ, Sheppard MN, Elliott PM, Pennell DJ, Prasad SK (2010) Prognostic significance of myocardial fibrosis in hypertrophic cardiomyopathy. J Am Coll Cardiol 56:867–874

28. Padiyath A, Gribben P, Abraham JR, Li L, Rangamani S, Schuster A, Dandord DA, Pedrizzetti G, Kutty S (2012) Echocardiography and cardiac magnetic resonance-based feature tracking in the assessment of myocardial mechanics in tetralogy of Fallot: an intermodality comparison. Echocardiography 30:203–210

29. Popovic ZB, Kwon DH, Mishra M, Buakhamsri A, Greenberg NL, Thamilarsan M, Flamm SD, Thomas JD, Lever HM, Desai MY (2008) Association between regional ventricular function and myocardial fibrosis in hypertrophic cardiomyopathy assessed by speckle tracking echocardiography and delayed hyperenhancement magnetic resonance imaging. J Am Soc Echocardiogr 21:1299–1305

30. Puchalski MD, Williams RV, Askovich B, Sower CT, Hor KH, Su JT, Pack N, Dibella E, Gottliebson WM (2009) Late gadolinium enhancement: precursor to cardiomyopathy in Duchenne muscular dystrophy. Int J Cardiovasc Imaging 25(1):57–63

31. Satio M, Okayama H, Yoshii T, Higashi H, Morioka H, Hiasa G, Sumimoto T, Inaba S, Nishimura K, Inoue K, Ogimoto A, Shigematsu Y, Hamada M, Higaki J (2012) Clinical significance of global two-dimensional strain as a surrogate parameter of myocardial fibrosis and cardiac events in patients with hypertrophic cardiomyopathy. Eur Heart J Cardiovasc Imaging 13:617–623

32. Schuster A, Kutty S, Padiyath A, Parish V, Gribben P, Danford DA, Makowski MR, Bigalke B, Beerbaum P, Nagel E (2011) Cardiovascular magnetic resonance myocardial feature tracking detects quantitative wall motion during dobutamine stress. J Cardiovasc Magn Resonan 13:58

33. Schuster A, Paul M, Bettencourt N, Morton G, Chiribiri A, Ishida M, Hussain S, Jogiya R, Kutty S, Bigalke B, Perera D, Nagel E (2013) Cardiovascular magnetic resonance myocardial feature tracking for quantitative viability assessment in ischemic cardiomyopathy. Int J Cardiol 166(2):413–420

34. Sengupta PP, Mehta V, Arora R, Mohan JC, Khandheria BK (2005) Quantification of regional nonuniformity and paradoxical intramural mechanics in hypertrophic cardiomyopathy by high frame rate ultrasound myocardial strain mapping. J Am Soc Echocardiogr 18:737–742

35. Serri K, Reant P, Lafitte M, Berhouet M, Bouffos VL, Roudaut R, Lafitte S (2006) Global and regional myocardial function quantification by two-dimensional strain. Application in hypertrophic cardiomyopathy. J Am Coll Cardiol 47(6):1175–1181

36. Shirani J, Pick R, Roberts WC, Maron BJ (2000) Morphology and significance of the left ventricular collagen network in young patients with hypertrophic cardiomyopathy and sudden cardiac death. J Am Coll Cardiology 35:36–44

37. Smith BM, Dorfman AL, Yu S, Agarwal PP, Mahani MG, Lu JC (2007) Clinical significance of late gadolinium enhancement in pediatric patients with hypertrophic cardiomyopathy. Rev Esp Cardiol 60:15–23

38. Smith BM, Dorfman AL, Yu S, Russell MW, Agarwal P, Mahani MG, Lu JC (2014) Clinical significance of late gadolinium enhancement in patients <20 years of age with hypertrophic cardiomyopathy. Am J Cardiol 113:1234–1239

39. Taylor RJ, Moody WE, Umar F, Edwards NC, Taylor TJ, Stegemann B, Townend JN, Hor KN, Steeds RP, Mazur W, Levya F (2015) Myocardial strain measurement with feature-tracking cardiovascular magnetic resonance: normal values. Eur Heart J Cardiovasc Imaging 16(8):871–881

40. Varnava AM, Elliott PM, Sharma S, Mckenna WJ, Davies MJ (2000) Hypertrophic cardiomyopathy: the interrelation of disarray, fibrosis, and small vessel disease. Heart 84:476–482

41. Varnava AM, Elliott PM, Mahon N, Davies MJ, Mckenna WJ (2001) Relation between myocyte disarray and outcome in hypertrophic cardiomyopathy. Am J Cardiol 88:275–279

42. Weidemann F, Mertens L, Gewillig M, Sutherland GR (2001) Quantification of localized abnormal deformation in asymmetric nonobstructive hypertrophic cardiomyopathy: a velocity, strain rate, and strain Doppler myocardial imaging study. Pediatr Cardiol 22:534–537

43. Yang H, Sun JP, Lever HM, Popovic ZB, Drinko JK, Greenberg NL et al (2003) Use of strain imaging in detecting segmental dysfunction in patients with hypertrophic cardiomyopathy. J Am Soc Echocardiogr 16:233–239